J Radioanal Nucl Chem (2017) 312:531–541
DOI 10.1007/s10967-017-5261-7

Kinetics and pH-dependent uranium bioprecipitation by *Shewanella putrefaciens* under aerobic conditions

Wenbo Huang[1] · Xiaoqin Nie[1] · Faqin Dong[2] · Congcong Ding[1] · Rong Huang[1] · Yilin Qin[3] · Mingxue Liu[3] · Shiyong Sun[2]

Received: 12 December 2016 / Published online: 29 April 2017

Abstract The removal behavior of U(VI) by *Shewanella putrefaciens* was investigated in this study. Our results demonstrated the formation of uranium phosphate biomineral, predominantly existed as chernikovite [$H_2(UO_2)_2(PO_4)_2{\cdot}8H_2O$], on the cell surface of *S. putrefaciens*. The lamellar chernikovite was found at slightly acid pH, but not at pH > 7.0. Phosphate-containing groups played the key role in the formation of chernikovite based on the analysis of IR. After ashing and hydrothermal process, bacterially mediated chernikovite can be transformed into inorganic uranium phosphate and UO_2, respectively. The findings can provide a potential strategy for in situ bioremediation of uranium in aerobic environment.

Graphical abstract Biomineralization process of uranium on *S. putrefaciens*.

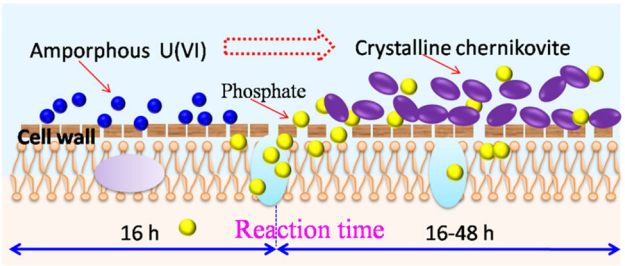

Biomineralization process of uranium on *S. putrefaciens*

Keywords Uranium · *Shewanella putrefaciens* · Biomineralization · Chernikovite

Introduction

Uranium contamination in groundwater and soils poses a significant environmental problem at current and former uranium mining or nuclear facilities. Uranium is predominantly as highly soluble hexavalent uranium [U(VI)] in oxidizing environment, i.e. uranyl ion $\left(UO_2^{2+}\right)$ or hydroxyl complexes below ~pH 6.5, or uranyl carbonate complexes at higher pH [1]. The radioactive and toxic U(VI) is more prone to migrate in near-surface water and groundwater, threatening the environmental safety and human health [2, 3]. Therefore, it has been an emergent issue to remediate the uranium contaminated water to acceptable levels.

Microbe-based systems are increasingly viewed as potentially useful approaches for bioremediation in situ and for radionuclide biorecovery, due to the low-cost, simple design, high feasibility, and environmental friendly

✉ Xiaoqin Nie
xiaoqin_nie@163.com

✉ Congcong Ding
dingc_3650483@163.com

[1] Fundamental Science on Nuclear Wastes and Environmental Safety Laboratory, Southwest University of Science and Technology, Mianyang 621010, People's Republic of China

[2] Key Laboratory of Solid Waste Treatment and Resource Recycle, Ministry of Education, Southwest University of Science and Technology, Mianyang 621010, People's Republic of China

[3] School of Life Science and Engineering, Southwest University of Science and Technology, Mianyang 621010, People's Republic of China

property [4]. Microbe is widespread in environment, and possesses characters such as good tolerance to harsh environment, high surface-to-volume ratio and abundant functional groups, which contributes to immobilization of metal ions [5–11]. There have been extensive studies done on the biosorption and bioaccumulation of uranium by microbes under different environmental conditions [3, 4, 6]. Some microbes were also reported to alter the speciation and mobility of radionuclides via the biomineralization process, precipitating uranium through complexation with anions [12]. Bacterial cells covering entire uranium phosphate minerals have been observed in natural uranium-containing soils, suggesting the important role of bacteria in forming mineral phase of uranium [13]. As previous research has demonstrated, many microorganisms can accumulate large amounts of toxic metals and generate crystalline minerals: metals can precipitate with ligands generated from chemical and/or enzymatic processes [14, 15]. Gadd et al. [12]. reported that radionuclide related oxides, phosphates, sulfides and oxalates are the most common biominerals precipitated by microbes. *Citrobacter* sp. can induce the formation of U(VI)-phosphate minerals as a result of phosphatase-mediated hydrolysis of an organic source of phosphorus in the presence of U(VI) [16, 17]. Liang et al. [18] found that several yeast strains can accumulate and immobilize uranium through phosphatase-faciliated uranium phosphate precipitation. Dead biota and derived products may also provide a template for mineral deposition under particular physic-chemical conditions [12]. The uranium phosphate minerals have been regarded as a more durable process than adsorbed uranium since insoluble minerals can remain in an insoluble state even after cell lysis [19].Uranium biominerals (i.e. uranium sulfide/phosphate mineral) precipitated by microbes can be capable of long term uranium retention, because they are insoluble and not sensitive to oxygen change [12]. The longevity of uranium biomineral has been demonstrated in natural analogue sites [20–22]. Thus, fundamental understanding of uranium biomineralization process under different environmental conditions is helpful for developing short- and long-term radioactive waste treatment strategies.

Shewanella putrefaciens (*S. putrefaciens*), a facultatively anaerobic bacteria, was chosen in this study. Previous studies on the bioremediation of uranium have primarily focused on reducing U(VI) to U(IV) [23, 24]. However, biogenic U(IV) has been found susceptible to oxidative remobilization after exposure to oxygen or nitrate [25, 26], and therefore may not be an ideal end-product for a long-term in situ remediation strategy. Additionally, much of uranium contamination is in vadose zone where aerobic conditions prevail [27]. Interestingly, few studies, as far as we are aware, are available on the biomineralization of uranium by *S. putrefaciens* in aerobic conditions. Besides, the hydrothermal and ashing treatments were used in this study to investigate the phase transformation of bacterially mediated uranium mineral, which is vital to the recovery of uranium.

The objectives of this study are: (1) to investigate the immobilization behavior of U(VI) on *S. putrefaciens* under various environmental conditions (i.e. pH, contact time, the concentration of U(VI) and bacteria) by batch techniques in aerobic environment; (2) to identify the chemical composition of uranium mineral formed during biomineralization; (3) to explore the biomineralization mechanism using X-ray diffraction (XRD), infrared spectroscopy (IR) and scanning electron microscopy and energy dispersive X-ray spectrometry (SEM–EDS) techniques. We are interested in how pH and contact time influenced the uranium biomineralization process mediated by *S. putrefaciens*.

Material and method

Materials

All chemicals used in this study were analytical grade, and all solutions were prepared using Milli-Q water. The *S. putrefaciens* strain was purchased from China Center of Industrial Culture Collection (CICC 22,940). *S. putrefaciens* cells were cultured in sterilized medium (tryptone, 15 g; yeast extract, 5 g; sodium chloride, 5 g; H_2O, 1 L) at 30 °C. Next, the cells were harvested by centrifugation (6000 rpm, 10 min) after 48 h and were washed three times using NaCl solutions (0.9%, mass percent).Aliquots of the harvested cells were prepared through autoclaving (121 °C, 20 min) as dead cells. The U(VI) stock solution (1.0 g/L) was prepared from $UO_2(NO_3)_2{\cdot}6H_2O$ in a 0.01 M HNO_3 solution.

Bach experiment

Batch experiment was conducted with 0.37 g/L *S. putrefaciens* and 100 mg/L U(VI) solution at $T = 30$ °C. Briefly, 1.5 mL of U(VI) stock solution (1.0 g/L) was added to the polypropylene tubes containing 13.5 mL *S. putrefaciens* cell suspensions containing 0.9% NaCl. Next, the suspensions were sealed and continuously stirred (150 r/min) at 30 °C. To minimize the effect of the radionuclide adsorption on the tube walls, the sorption of U(VI) without bacterial cells was carried out under the same experimental conditions. The pH values were adjusted to be in the range 3.0–8.0 by adding negligible volumes of 1.0 mol/L Na_2CO_3 and HCl. Except from pH-dependent sorption experiment, other experiments were conducted at pH 5.0 since the highest U(VI) removal was found at this pH value. After 24 h (enough for the equilibrium) of shaking at 30 °C, the suspensions were centrifuged at 6000 rmp for 10 min. The

concentrations of U(VI) in supernatant were determined by a ultraviolet pulse trace uranium analyzer (WGJ-III, China).Nine tubes containing the suspensions were conducted with the same experimental conditions, andthe supernatant was periodically separated from the independent tube for kinetics experiment.

Removal percentage (R) and removal capacity [Q (mg/g)] can be expressed as Eqs. (1) and (2), respectively:

$$R = (C_0 - C_e)/C_0 \times 100\% \quad (1)$$

$$Q = V \times (C_0 - C_e)/m \quad (2)$$

where C_0 (mg/L) and C_e (mg/L) are initial concentration and concentration after sorption, respectively. m (g) and V (mL) are the mass of *S. putrefaciens* and the volume of the suspension, respectively. All of the experimental data were averages of triplicate data (the resulting error bars (within ±5%) are provided).

Hydrothermal and ashing treatment

Hydrothermal and ashing treatment were conducted to evaluate the recovery of uranium immobilized by *S. putrefaciens* and the phase transition of U-phosphate mineral. Uranium-loaded *S. putrefaciens* cells were collected after the equilibrium of above sorption experiment at 100 mg/L U(VI). For hydrothermal treatment, the uranium-free and uranium-loaded *S. putrefaciens* cells were added into a 50 mL Teflon-lined stainless steel autoclave. Next, the Teflon-lined stainless steel autoclave was reacted at 200 °C for 48 h. The ashing treatment was performed according to the method of Liu et al. [28]. The uranium-loaded *S. putrefaciens* cells were collected after equilibrium of sorption experiment with 0.37 g/L *S. putrefaciens* and 100 mg/L U(VI) solution at $T = 30$ °C. The collected cells were washed with Milli-Q water for three times and then dried at 55 ± 0.5 °C. 2.5 g dried uranium-loaded cells were ashed at 650 °C for 4 h, and last obtained 0.37 g ashing products.

Characterization

S. putrefaciens cells before and after 100 mg/L U(VI) sorption were characterized by XPS, SEM, IR, and XRD techniques. Samples for SEM analysis were firstly fixed with 2.5% glutaraldehyde solution for 12 h, and then dehydrated in graded concentrations of ethanol (30, 50, 70, 90 and 100%) for 20 min in turn. After that, samples were air-dried and sputter-coated with gold particles. Finally, the gold-covered samples were examined on Ultra 55 SEM coupled with Oxford IE450X-Max80 EDS. IR spectra were obtained from a Perkin-Elmer Nicolet-5700 spectrophotometer in the range of 4000–400 cm^{-1} and in the resolution ratio of 4 cm^{-1} using the KBr disc technique. Samples were mixed with sufficient KBr (approximately with the ratio of 1/40) and fully grinded. IR spectra were post-processed using the Bruker OPUS 6.5. A Thermo Escalab 250 XPS was conducted at 150 W with Al Kα radiation. The energies were corrected by C 1 s peak at 284.6 eV as a reference. The XPS data were processed using the XPSPEAK software (version 4.1). The XRD analysis was recorded by a PANalytical X'Pert PRO diffractometer with Cu-Kα radiation ($\lambda = 1.5406$ Å). The voltage and electric current was 40 kV and 40 mA, respectively. The 2θ scanning ranged from 3 to 80° in steps of 0.0334225° with a count time of 10.16 s. The data was analyzed by the software of X'Pert High Score Plus, and the phase construction of U(VI) immobilized on *S. putrefaciens* was identified using the PDF-2 database of the International Center for Diffraction Data (ICDD).

Results and discussion

Effect of pH

The effect of pH on the immobilization of U(VI) by *S. putrefaciens* is shown in Fig. 1a. pH-dependent immobilization behavior was found: U(VI) removal increased with increasing pH from 3.0 to 5.0, but decreased with further increasing pH from pH 5.0 to pH 8.0. The maximum immobilization percentage of U(VI) (~90%) was obtained at pH 5.0. The control test (no bacteria added) reveals that U(VI) precipitation was not formed over investigated pH range from 3.0 to 8.0. The observed U(VI) removal trend might be explained by the U(VI) species varied with pH and the surface charge of bacteria. The isoelectric point value of bacteria was reported at generally below pH 3.0 [29], so the surface of *S. putrefaciens* was more negatively charged at pH > 3.0. Figure 1b described the distribution of U(VI) species in the presence of 14.56 mmol/L Na_2CO_3 (comparable to the maximum adding dosage for adjusting pH) among the investigated pH range, calculated by Visual MINTEQ 3.0. At pH 3.0–5.0, The positive or uncharged U(VI) species [i.e. $\left(UO_2^{2+}\right)$, $(UO_2)_2(OH)_2^{2+}$ or UO_2CO_3] dominated, and favored the sorption onto the negatively charged cell surface. However, negative U(VI) species like $UO_2(CO_3)_2^{2-}$ and $UO(CO_3)_3^{4-}$ rose with increasing pH from 5.0 to 8.0. Thus, the decreased U(VI) immobilization on *S. putrefaciens*at pH > 5.0 might be due to the electrostatic repulsion between negative *S. putrefaciens* and negative U(VI) species. Compared with the sorption behavior of other bacteria under carbonate-absent conditions [30], the immobilized U(VI) amounts on *S. putrefaciens* under carbonate-present conditions are greatly decreased at higher pH, suggesting that carbonate greatly influences the sorption of U(VI) at alkaline pH. Actually,

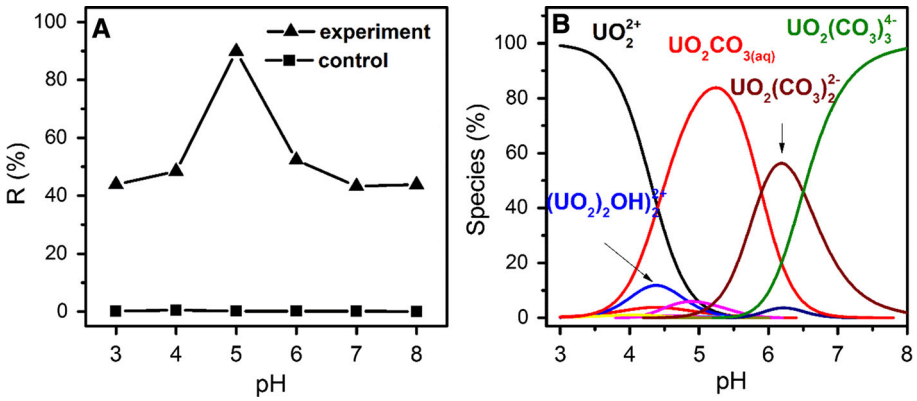

Fig. 1 **a** Effect of pH on the immobilization of U(VI) by *S. putrefaciens*, $C_{U(VI)} = 100$ mg/L, $t = 72$ h, $C_{bacteria} = 0.37$ g/L, $T = 30$ °C, **b** the distribution of U(VI) species *versus* pH calculated by Visual MINTEQ 3.0, $C_{Na_2CO_3} = 14.56$ mmol/L, $C_{U(VI)} = 100$ mg/L

uranium is dominant as uranyl carbonate complexes at pH > 7.0 in natural environments [1]. Kulkarni et al. [31] found that the cell-bound or extracellular location of uranium bioprecipitation was governed by the uranyl species present at carbonate-deficient/abundant conditions. Previous researchers determined that uranium biomineralization by microbes might undergo a two-stage step: sorption of U(VI) to cell surface as the first step, and subsequent uranium precipitation through complexation with the anions present in the system like phosphate anions [32, 33]. Thus, the favorable sorption of U(VI) on *S. putrefaciens*at weak acid pH was expected to lead to the high uranium precipitation amounts.

Effect of contact time

Figure 2 describes U(VI) removal on living and dead *S. putrefaciens* as a function of contact time. For the sorption behavior of living *S. putrefaciens* in Fig. 2a, an obvious two-stage U(VI) removal process was observed during the initial 24 h: the first 1–16 h phase with slower increase of 138.6 mg/g to 169.3 mg/g immobilized U(VI), and the second 16-24 h phase with rapidly increase immobilized U(VI) to 244.3 mg/g. After 24 h, the removal of U(VI) by *S. putrefaciens* reached the equilibrium state. The dead *S. putrefaciens* was investigated as a contrast, and its removal behavior did not present a similar two-stage sorption trend as a function of time (Fig. 2b).The sorption equilibrium was fast reached within 1 h for dead *S. putrefaciens*. The different sorption behavior between living and dead cells implies that microbial activity plays an important role in the immobilization of U(VI) by *S. putrefaciens*. For living *S. putrefaciens*, uranium might be just adsorbed on the cell surface in the first stage by electrostatic forces or by complexing with carboxylic and phosphate groups in *S. putrefaciens*, which is agreement with the previous idea [32, 33]. Uranium complexation with both organic and inorganic might reduce its toxicity [4].The initial 16 h can be an adjustment moment for *S. putrefaciens* to adapt a new environment containing U(VI), i.e., the synthesis and conserve enzymes like phosphatase related to uranium detoxification. After the adjustment phase, massive phosphate ligands were released by *S. putrefaciens* as a result of phosphatase activity in the second phase from 16 to 24 h. Then, phosphate anions rapidly precipitates with U(VI)

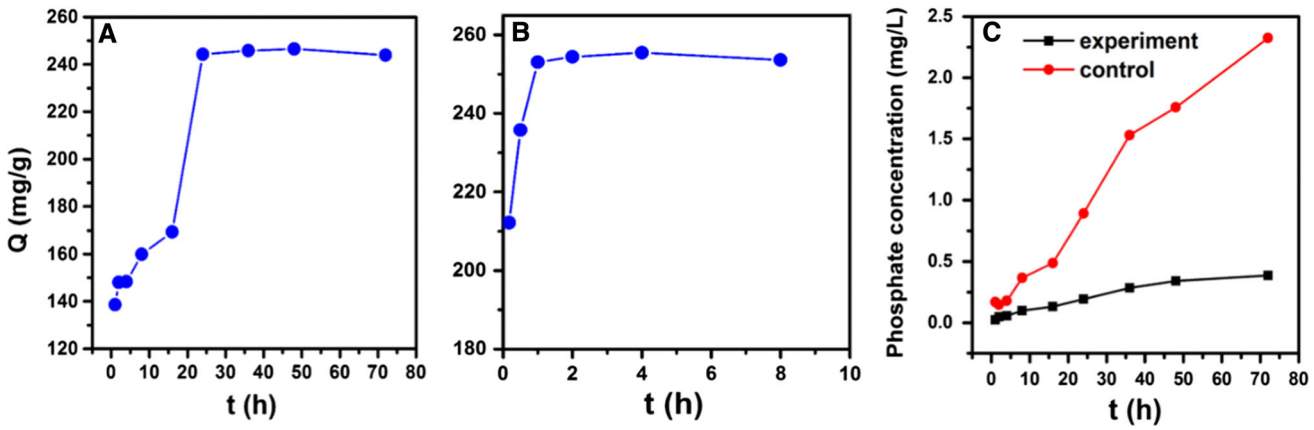

Fig. 2 Effect of contact time on U(VI) immobilization by living *S. putrefaciens* (**a**) and dead *S. putrefaciens* (**b**); the release of phosphate as a function of time for original and uranium-loaded *S. putrefaciens* (**c**); pH = 5.0, $C_{U(VI)} = 100$ mg/L, $C_{bacteria} = 0.37$ g/L, $T = 30$ °C

[16, 17]. The hypothesis is supported by the SEM images in Fig. 6 where the formation of uranium phosphate minerals occurred at 24 h but not at 8 h. Gorman-Lewis et al. [34] approved that uranium phosphate precipitation may be mediated by both electrostatic forces and binding to sites such as carboxylic and phosphate groups.

Figure 2c shows the concentration of phosphate released in solutions for the control and uranium-loaded samples at pH 5.0. Phosphate concentration was determined by vanadium molybdate blue colorimetric method [35]. There is an obvious difference for phosphate content between control group and experimental group in solution as a function of time. For the control group, the released phosphate increased with increasing time, especially after 16 h. However, phosphate concentration in solution was relatively low in experimental group. For example, the content of released phosphate was 2.32 and 0.39 mg/L for control and uranium-loaded sample, respectively at 72 h. The released phosphate combined with U(VI) to form U(VI)-phosphate precipitation, thus leading to less phosphate concentration in solution for the experimental group. The result reveals that *S. putrefaciens* can release large amounts of phosphate substances to outside cells, and the phosphate anions rapidly precipitates with U(VI).

Effects of *S. putrefaciens* and U(VI) concentrations

The effects of *S. putrefaciens* concentration on U(VI) removal are shown in Fig. 3a. U(VI) removal capacity per gram of bacteria increased from 198.5 to 237.6 mg/g with the increase of *S. putrefaciens* from 0.14 to 0.28 g/L, and then the removal capacity decreased with increasing bacteria concentration. Although the increase of *S. putrefaciens* would lead to the increased sorption sites, the concentration of U(VI) was fixed in the system. Thus, when *S. putrefaciens* concentration exceeded 0.28 g/L, the sorption sites were over-saturation for U(VI), and the removal capacity per unit mass decreased. For example, U(VI) removal capacity was 99.88 mg/g at 0.72 g/L *S. putrefaciens*. Although U(VI) removal percentage increased with the increase of *S. putrefaciens* concentration, the corresponding removal capacity decreased. Thus, the sorption sites provided by *S. putrefaciens* were oversaturated for U(VI), and the best bacteria utilization efficiency was not obtained. Figure 3b reveals the effect of initial U(VI) concentration on U(VI) immobilization by *S. putrefaciens* at pH 5.0. The immobilization capacity increased from 1 to 100 mg/L U(VI), and then the immobilization capacity was kept with increasing U(VI) concentration. The maximum U(VI) immobilization capacity was 244.3 mg/g at pH 5.0. The decreased U(VI) immobilization percentage was observed from 100 to 200 mg/L

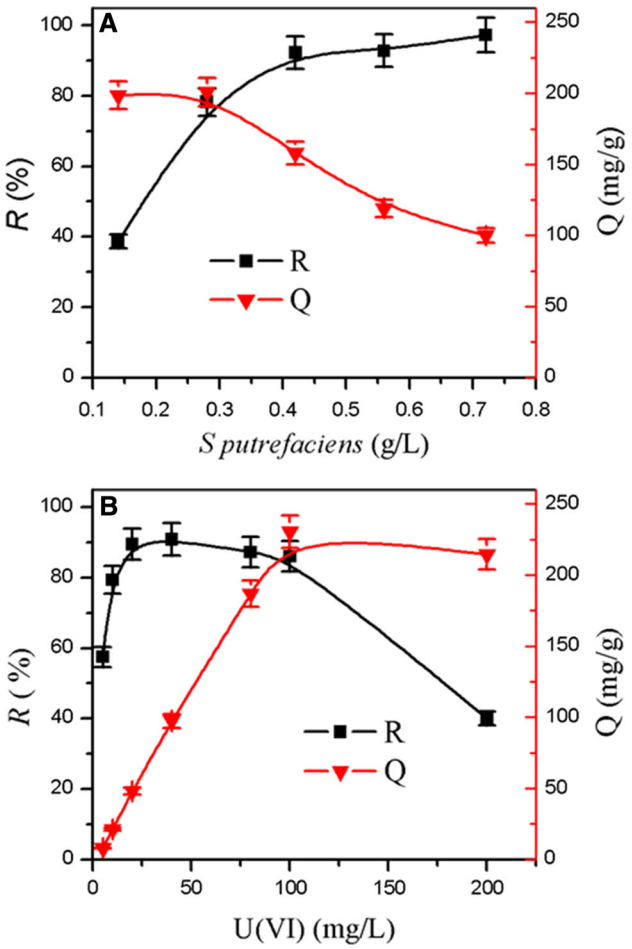

Fig. 3 Effect of *S. putrefaciens* concentration (**a**) and U(VI) concentration (**b**) on the immobilization of U(VI) at pH 5.0 and $T = 30$ °C

U(VI), suggesting that the amount of U(VI) was more than the saturated immobilization capacity of *S. putrefaciens*.

Solid-phase characterization

SEM–EDS analysis

Figure 4 shows the SEM images of original and uranium-loaded *S. putrefaciens* at pH 3.0, 5.0 and 8.0. The original *S. putrefaciens* exhibited intact shape and smooth surface. In contrast to the original bacteria, there was lots of lamellar precipitation with a diameter of ~500 nm in the surrounding or on the surface of uranium-loaded *S. putrefaciens* at pH 3.0 and 5.0, but not on the ones at pH 8.0. Similar precipitation was found by Nie et al. [36] on the root cells of *Spirodela punctata* after U(VI) sorption. By comparison, more precipitate was observed in the surrounding of bacteria at pH 3.0, while the lamellar precipitate was predominantly present on the surface of bacteria at pH 5.0, covering the whole *S. putrefaciens* with a

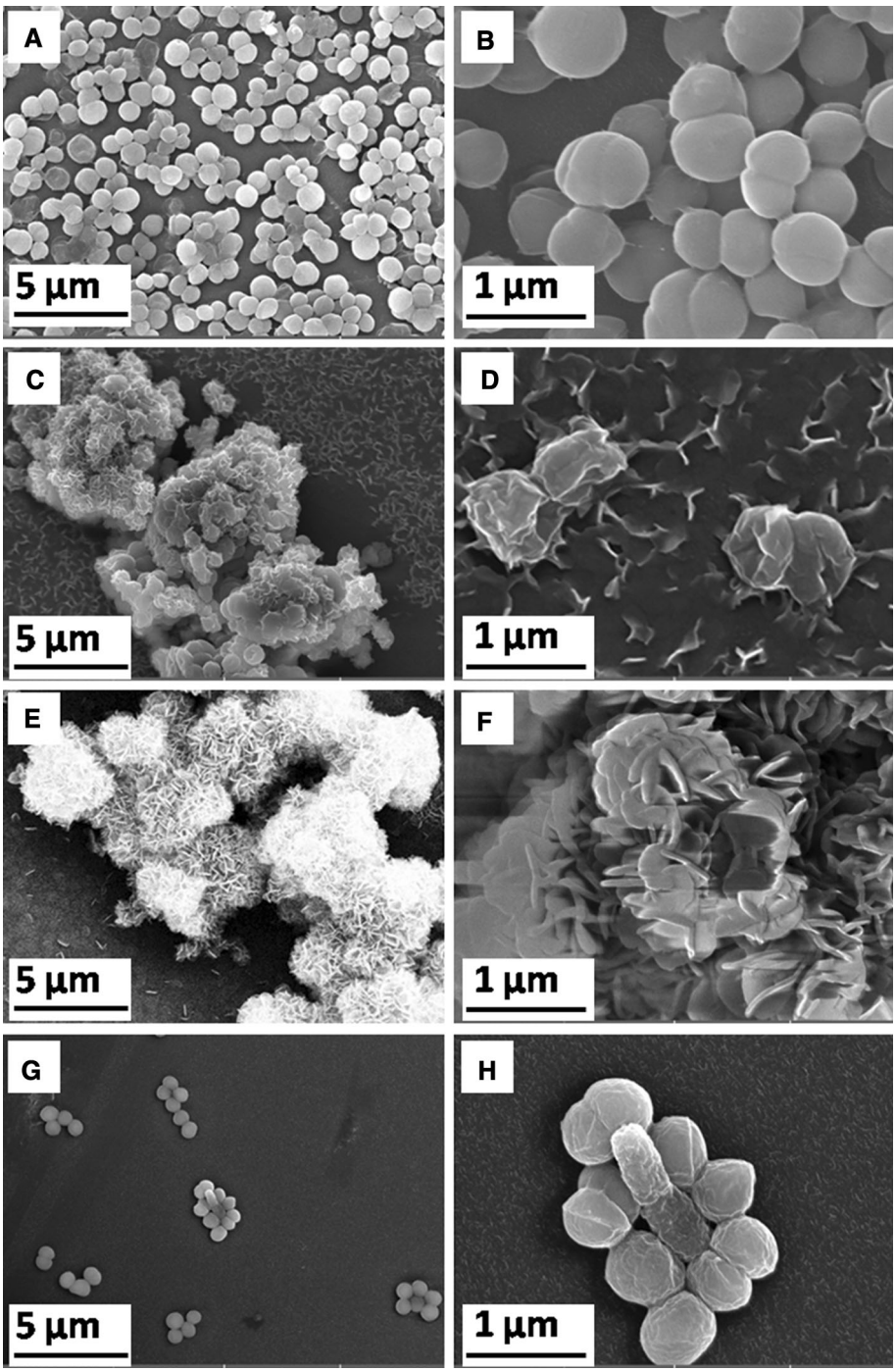

Fig. 4 SEM images of original *S. putrefaciens* (**a**, **b**) and uranium-loaded *S. putrefaciens* at pH 3.0 (**c**, **d**), pH 5.0 (**e**, **f**) and pH 8.0 (**g**, **h**), $C_{U(VI)} = 100$ mg/L and $t = 24$ h

hedgehog-like shape. The EDS spectrum at pH 5.0 exhibited obvious U peaks and the increased P peaks of uranium-loaded *S. putrefaciens* compared with that of original *S. putrefacien* (Fig. 5). According to the results in Fig. 3c, the original *S. putrefaciens* released phosphate to solutions, whereas the released phosphate coordinated with U(VI) to form stable precipitation for uranium-loaded *S. putrefaciens*. Thus, EDS spectrum derived from the lamellar precipitation exhibited significantly higher content P relative to original *S. putrefaciens*. Additionally, the decreased intensity of Si peaks for uranium-loaded *S. putrefaciens* might be attributed to the aggregated bacteria after reaction with U(VI), which led to less X-ray on cover glass. XRD results further demonstrated the lamellar precipitation as crystalline uranium phosphate compounds. Uranium precipitates occurred due to phosphate release from the cellular polyphosphate, likely as a response of cell to added uranium [37]. Phosphatase activity is a

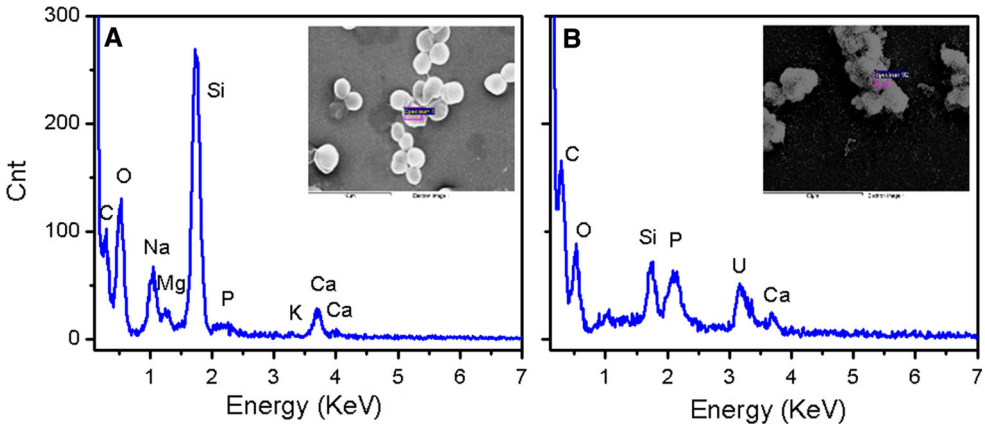

Fig. 5 EDS spectra of original *S. putrefaciens* (**a**) and uranium-loaded *S. putrefaciens* at pH 5.0

characteristic common to most bacteria, since phosphorus is an essential nutrient. The important role of phosphatase enzyme has been demonstrated in the uranium phosphate biomineralization [38, 39]. It has been reported that some bacteria can liberate phosphate to outside of cells, and then the released phosphate induced precipitation of uranium [38, 40]. However, Sousa et al. [41] observed the U-phosphate precipitation inside the bacterial cells, and they determined that phosphate was accumulated inside the cells instead of released into extracellular matrix. The uranium biomineralization not only depends on uranium sorption, but also the release of free phosphate as a result of phosphatase activity [42, 43].

SEM analysis revealed that the most favorable uranium phosphate precipitation occurred at pH 5.0, which is consistent with the batch experiment result. The precipitation of uranium was relatively less at pH 3.0, which might be due to the double stress of low pH and uranium toxicity, leading to the low sorption of U(VI) and low metabolic activity of bacteria [43]. The absence of uranium precipitate at pH 8.0 might be attributed to the low sorption of U(VI). Thermodynamic modeling in Fig. 1b predicted that U(VI) species were predominantly as negative carbonate uranyl complexes at pH $>$ 7.0, more stable in solutions but unfavorable adsorbed. Thermodynamically, carbonate could influence the solubility of the precipitated U(VI) mineral at higher pH [38]. The SEM results *versus* pH implies that high sorption of U(VI) onto *S. putrefaciens* leads to the occurrence of uranium biomineralization.

Figure 6 shows the SEM images of *S. putrefaciens* exposed to U(VI) solutions after 8, 24, and 48 h. The uranium phosphate precipitation was almost not observed for *S. putrefaciens* after 8 h (Fig. 6a, d), while the precipitation was obviously seen on or around the bacteria after 24 (Fig. 6b, e) and 48 h (c, f). The absence of uranium biominerals at 8 h suggested U(VI) was adsorbed via electrostatic attraction or covalent binding functional groups in the cells. As the discussion in time-dependent experiment, *S. putrefaciens* mainly conducted extracellular activities at the initial time (<16 h) to adapt the uranium-added environment, including chemical communication, gene regulation, and phosphatase expression and so on. The U-phosphate precipitation occurred at prolonged U(VI) contact (24–48 h), which can be attributed to the increased phosphate concentration generated by phosphatase. Interestingly, the distribution *S. putrefaciens* is relatively dispersive at 8 h, while *S. putrefaciens* tended to be flocculated together, which might be a resistant mechanism from uranium-contaminated environment. Our SEM results support that formation of uranium biominerals was mediated by the first sorption of U(VI) on *S. putrefacien*.

XPS analysis

XPS was used to determine the valence states of uranium precipitation on the *S. putrefaciens* surface. Figure 7a shows the total scans of XPS spectra for control and uranium-loaded samples at pH 5.0. The presence of characteristic peak of U 4f after sorption demonstrates the high accumulation ability of *S. putrefaciens*. The deconvoluted $U4f_{7/2}$ (381.66 eV) and $U4f_{5/2}$ (392.58 eV) XPS spectra are shown in Fig. 7b. U 4f spectrum could be satisfactorily fitted by U(IV) at 379.90 and 391.39 eV and U(VI) at 381.63 and 392.59 eV [44], which suggests that part of U(VI) was reduced to U(IV) by *S. putrefaciens*. However, the amount of U(IV) on *S. putrefaciens* was significantly less than that of U(VI). Thus, uranium was predominantly existed as U(VI) on *S. putrefaciens*.

IR analysis

Figure 7c shows IR spectra of *S. putrefaciens* without or with U(VI) treatment at different pH from 2000 to 400 cm^{-1}. The control sample exhibited the characteristic peaks of microorganisms, i.e. amide I at 1652 cm^{-1}, amide II at 1543 cm^{-1}, $–CH_2$ or CH_3 peaks at 1477 cm^{-1}, and the

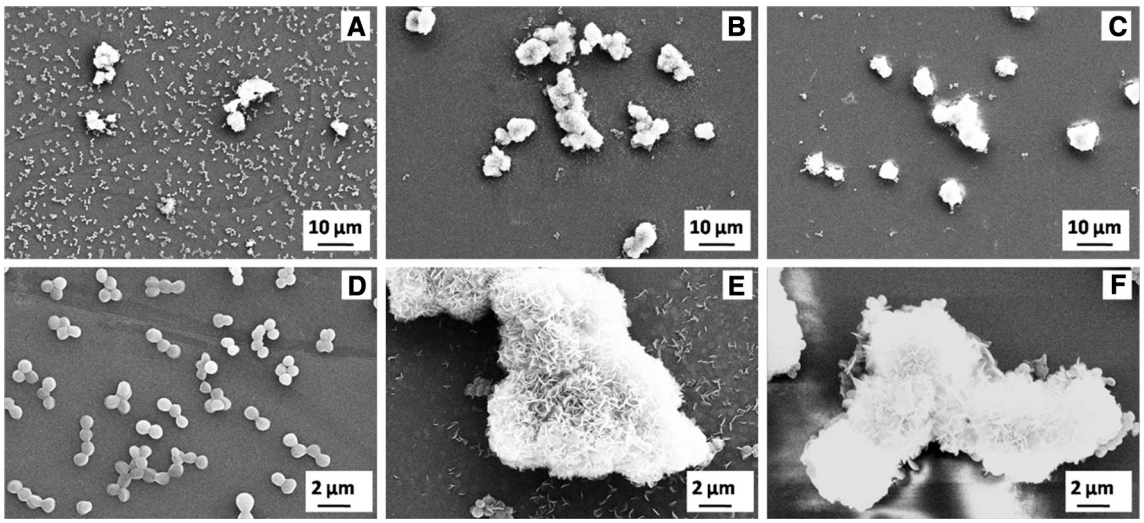

Fig. 6 SEM images of uranium-loaded *S. putrefaciens* at 8 h (**a**, **d**), 24 h (**b**, **e**), and 48 h (**c**, **f**), $C_{U(VI)} = 100$ mg/L

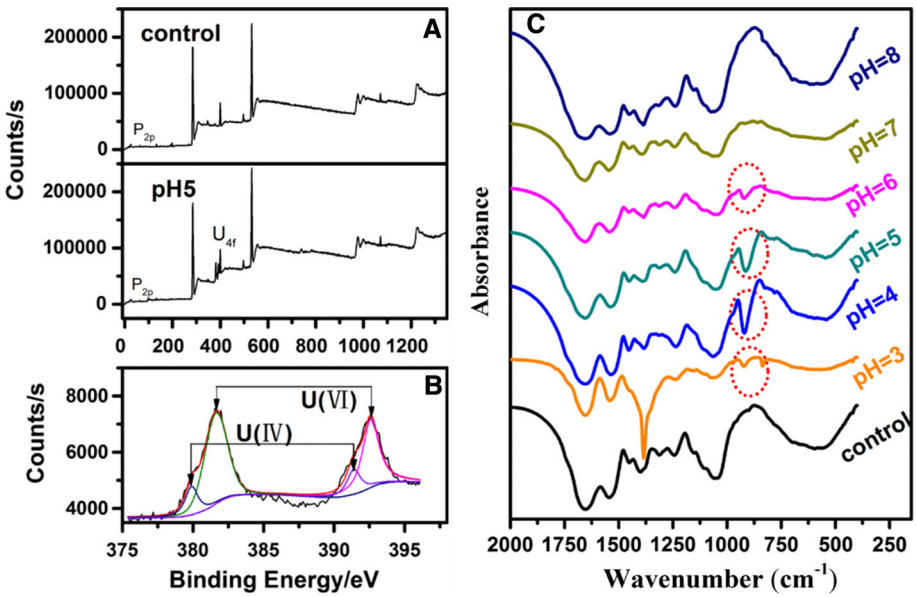

Fig. 7 **a** Full scan of *S. putrefaciens* before and after U(VI) treatment at pH 5.0, **b** U4f spectrum of U(VI)-load *S. putrefaciens*, **c** IR spectra of *S. putrefaciens* before and after U(VI) treatment at different pH value, $C_{U(VI)} = 100$ mg/L, $t = 24$ h

phosphate asymmetric and symmetric stretching bands between approximately 850 and 1200 cm^{-1} [45–47]. By comparison, the unique peak between 1500 and 1250 cm^{-1} at pH 3.0 might be attributed to the –OH of protonated –COOH groups. This band disappeared with increase of pH as a result of dissociation. After U(VI) treatment, $\upsilon_3(UO_2)$ mode at 922, 920, 914 and 921 cm^{-1} was observed at pH 3.0, 4.0, 5.0 and 6.0, respectively, representinga mix of monomeric, polymeric or carbonate containing hydroxy U(VI) complexes [48]. No $\upsilon_3(UO_2)$ mode was observed at pH 7.0 and 8.0, which might result from the less immobilized U(VI) amounts. Interestingly, $\upsilon_3(UO_2)$ mode occurring was shifted to lower frequency at pH 5.0, suggesting that the U(VI) surface species was different from that at pH 3.0, 4.0 and 6.0. This might be interpreted in terms of the formation of plenty of precipitated U(VI)-phosphate species at pH 5.0. The downshifts of the $\upsilon_3(UO_2)$ mode has been spectroscopically evidenced as a formation of inner-sphere complexes [49–51]. The strong peak at 1055 cm^{-1} belonged to symmetrical stretching vibration of the phosphates group ($-PO_4^{3-}$) [47]. The band of U(VI)-loaded *S. putrefaciens* showed a considerably increased half-width and a decreased intensity in comparison to the bands of original *S. putrefaciens*, suggesting an important role of phosphates groups in the immobilization of U(VI).

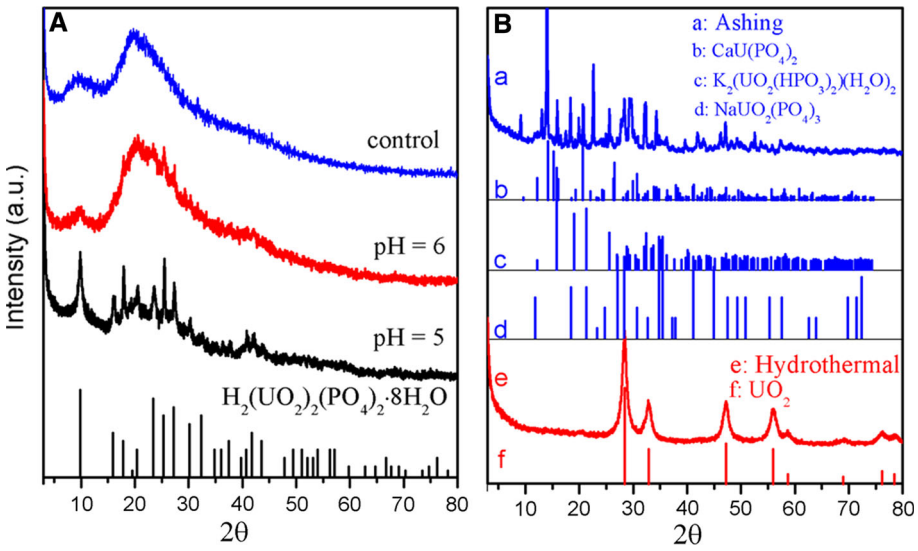

Fig. 8 **a** XRD pattern of original and uranium-loaded *S. putrefaciens* at pH 5.0 and 6.0, $C_{U(VI)} = 100$ mg/L, **b** XRD pattern of uranium-loaded *S. putrefaciens* after hydrothermal and ashing treatment at pH 5.0, $C_{U(VI)} = 100$ mg/L

XRD analysis

XRD was used to identify the chemical nature of U(VI) immobilized by *S. putrefaciens* in oxic conditions at pH 5.0 and 6.0 (Fig. 8a). A broad peak around $2\theta = \sim 20^{\circ}$ on the control sample indicated the pure *S. putrefaciens* was amorphous [50, 52]. However, obvious diffraction peaks, corresponding to $[H_2(UO_2)_2(PO_4)_2 \cdot 8H_2O]$ (PDF-2 00-008-0296), were observed on the bacteria cells in the presence of U(VI) at pH 5.0 and 6.0. Thus, the crystallized uranium product can be identified as a chernikovite. The characteristic diffraction peaks of chernikovite were more intense at pH 5.0 than pH 6.0, suggesting that more U-phosphate minerals were formed at pH 5.0, which is consistent with the macroscopic experiment. Additionally, the crystallized uranium product was not detected at pH 3.0, 4.0, 7.0 and 8.0 (data not shown). It might be the low abundance of U(VI)-phosphate minerals at acid pH, as evidenced by the SEM images, that failed to be detected by the detected by XRD technique. Suzuki and Banfield [43] found that $H_2PO_4^-$ and HPO_4^{2-}, as dominant species at pH 5.0, can favorably coordinate with uranyl ions, whereas the partial protonation of phosphate below pH 5.0 could lead to the decreased uranyl precipitation. Combination of SEM and IR analysis, we tended to determine that U(VI) was coordinated with functional groups on *S. putrefaciens* to form amorphous complexes at basic pH. This U-phosphate mineralization behavior was similar to previous finding by Paterson-Beedle et al. [53] who found that bacterial phosphatase activity hydrolyzed organophosphates and liberated inorganic phosphate to precipitate with aqueous U(VI) as hydrogen uranyl phosphate $(H_2(UO_2)_2(PO_4) \cdot_2 \cdot 8H_2O)$ minerals. However, Pan's work found the amorphous uranium compound could be transformed into crystalline nano-uramphite $(NH_4(UO_2)(PO_4) \cdot 3H_2O)$ by *B. thuringiensis* [54]. The XRD results indicated that *S. putrefaciens* would facilitate nucleation and precipitation of U(VI) in a crystalline state at slightly acidic pH.

Figure 8B reveals the XRD patterns of uranium-loaded *S. putrefaciens* (pH 5.0) after hydrothermal and ashing treatment. The diffraction peaks of hydrothermal products were highly coincident with that of characteristic uranium dioxide nanoparticles $[UO_2]$ (PDF-201-075-0420), suggesting that the U(VI) (chernikovite on *S. putrefaciens*) were transformed to U(IV) (UO_2) after hydrothermal treatment. After ashing treatment, the crystallite products of uranium on *S. putrefaciens* at pH 5 was transformed to more stable inorganic uranium phosphate phases, which can be well indexed as $K_2(UO_2(HPO_3)_2)(H_2O)_2$ (PDF-01-078-1339), $NaUO_2(PO_4)_3$ (PDF-00-034-1447), and $CaU(PO_4)_2$ (PDF- 01-086-0687).

Conclusion

The bacterially mediated U(VI) biomineralization, more stable to oxygen over a wide pH range, will be a complementary approach to anaerobic bioreduction in aerobic environments. This study demonstrates that *S. putrefaciens* can immobilize uranium as a chernikovite structure under aerobic conditions through the precipitation of phosphate with U(VI). The maximum U(VI) immobilization could be achieved to 244.3 mg/g at pH 5.0. The uranium phosphate biomineralization was the prevalent U(VI) immobilization mechanism for *S. putrefaciens* at slightly acidic environments. U(VI)-phosphate mineral significantly formed after 24 h contact with U(VI). We primarily find that the sorption of U(VI) mediates the occurrence of uranium biominerals.Our current findings prove a potential role of bacteria in biomineralization of uranium in aerobic aquifers

(i.e. vadose zone) below circumneutral pH. Further work is ongoing to determine the related metabolins of *S. putrefaciens* and their response mechanisms during uranium biomineralization, thus giving a thorough explanation of the formed uranium biominerals.

Acknowledgements This work was supported by the National Basic Research Program of China (973 Program: 2014CB846003), the China National Natural Science Foundation (Grant number: 41502316, 41672039), the Doctor Foundation of Southwest University of Science and Technology (Grant number: 15zx7109), the Prior Research Foundation of Fundamental Science on Nuclear Waste and Environmental Security Laboratory (Grant number: 15yyhk11), and the Undergraduate Innovation Fund Project by Southwest University of Science and Technology (CX16-021).

References

1. YiZ J, Yao J, ZhuMJ ChenHI, Wang F, Yuan ZM, Liu X (2016) Batch study of uranium biosorption by *Elodea canadensis* biomass. J Radioanal Nucl Chem 310:505–513
2. Ding C, Cheng W, Jin Z, Sun Y (2015) Plasma synthesis of beta-cyclodextrin/$Al(OH)_{(3)}$ composites as adsorbents for removal of UO_2^{2+} from aqueous solutions. J Mol Liq 207:224–230
3. Ding CC, Cheng WC, Sun YB, Wang XK (2015) Effects of Bacillus subtilis on the reduction of U(VI) by nano-Fe^0. Geochim Cosmochim Acta 165:86–107
4. Newsome L, Morris K, Lloyd JR (2014) The biogeochemistry and bioremediation of uranium and other priority radionuclides. Chem Geol 363:164–184
5. Ding CC, Feng S, Li XL, Liao JL, Yang YY, An Z, Wu QQ, Zhang D, Yang JJ, Tang J, Zhang J, Liu N (2014) Mechanism of thorium biosorption by the cells of the soil fungal isolate *Geotrichum* sp dwc-1. Radiochim Acta 102:175–184
6. Sun YB, Zhang R, Ding CC, Wang XX, Cheng WC, Chen CL, Wang XK (2016) Adsorption of U(VI) on sericite in the presence of *Bacillus subtilis*: a combined batch, EXAFS and modeling techniques. Geochim Cosmochim Acta 180:51–65
7. Yi ZJ, Yao J (2012) Kinetic and equilibrium study of uranium(VI) adsorption by *Bacillus licheniformis*. J Radioanal Nucl Chem 293:907–914
8. Ding CC, Cheng WC, Sun YB, Wang XK (2015) Novel fungus-Fe_3O_4 bio-nanocomposites as high performance adsorbents for the removal of radionuclides. J Hazard Mater 295:127–137
9. Cheng WC, Ding CC, Sun YB, Wang XK (2015) Fabrication of fungus/attapulgite composites and their removal of U(VI) from aqueous solution. Chem Eng J 269:1–8
10. Yi Z, Lian B (2012) Adsorption of U(VI) by *Bacillus mucilaginosus*. J Radioanal Nucl Chem 293:321–329
11. Ding CC, Feng S, Cheng WC, Zhang J, Li XL, Liao JL, Yang YY, An Z, Luo SZ, Yang JJ, Tang J, Liu N (2014) Biosorption behavior and mechanism of thorium on *Streptomyces sporoverrucosus* dwc-3.J. Radioanal Nucl Chem 301:237–245
12. Gadd GM, Pan X (2016) Biomineralization, bioremediation and biorecovery of toxic metals and radionuclides. Geomicrobiol J 33:175–178
13. Mondani L, Piette L, Christen R, Bachar D, Berthomieu C, Chapon V (2012) *Microbacterium lemovicicum* sp. nov., a bacterium isolated from a natural uranium-rich soil. Int J Syst Evol Microbiol 63:2600–2606
14. Gadd GM (2010) Metals, minerals and microbes: geomicrobiology and bioremediation. Microbiology 156:609–643
15. Kazy SK, Souza SF, Sar P (2009) Uranium and thorium sequestration by a *Pseudomonas* sp.: mechanism and chemical characterization. J Hazard Mater 163:65–72
16. Macaskie LE, Empson RM, Cheetham AK, Grey CP, Skarnulis AJ (1992) Uranium bioaccumulation by a *Citrobacter* sp. as a result of enzymically mediated growth of polycrystalline HUO_2PO_4. Science 257:782–784
17. Macaskie LE, Bonthrone KM, Rouch DA (1994) Phosphatase-mediated heavy metal accumulation by a *Citrobacter* sp. and related enterobacteria. FEMS Microbiol Lett 121:141–146
18. Liang X, Csetenyi L, Gadd GM (2016) Uranium bioprecipitation mediated by yeasts utilizing organic phosphorus substrates. Appl Microbiol Biotechnol 33:1–11
19. Ohnuki T, Ozaki T, Yoshida T, Sakamoto F, Kozai N, Wakai E, Francis AJ, Iefuji H (2005) Mechanisms of uranium mineralization by the yeast *Saccharomyces cerevisiae*. Geochim Cosmochim Acta 69:5307–5316
20. Pinto AJ, Gonçalves MA, Prazeres C, Astilleros JM, Batista MJ (2012) Mineral replacement reactions in naturally occurring hydrated uranyl phosphates from the Tarabau deposit: examples in the Cu–Ba uranyl phosphate system. Chem. Geol. s 312–313:18–26
21. Jerden JL, Sinha AK (2003) Phosphate based immobilization of uranium in an oxidizing bedrock aquifer. Appl Geochem 18:823–843
22. Jensen KA, Palenik CS, Ewing RC (2002) U6+ phases in the weathering zone of the Bangombé U-deposit: observed and predicted mineralogy. Radiochim Acta 90:761–769
23. Rui X, Kwon MJ, O'Loughlin EJ, Dunhamcheatham S, Fein JB, Bunker B, Kemner KM, Boyanov MI (2013) Bioreduction of hydrogen uranyl phosphate: mechanisms and U(IV) products. Environ Sci Technol 47:5668–5678
24. Cao B, Ahmed B, Kennedy DW, Wang Z, Shi L, Marshall MJ, Fredrickson JK, Isern NG, Majors PD, Beyenal H (2011) Contribution of extracellular polymeric substances from *Shewanella* sp. HRCR-1 biofilms to U(VI) immobilization. Environ Sci Technol 45:5483–5490
25. Moon HS, Komlos J, Jaffé PR (2007) Uranium reoxidation in previously bioreduced sediment by dissolved oxygen and nitrate. Environ Sci Technol 41:4587–4592
26. Senko JM, Istok JD, Suflita JM, Krumholz LR (2002) In-situ evidence for uranium immobilization and remobilization. Environ Sci Technol 36:1491–1496
27. Stubbs JE, Elbert DS, Veblen DR, Zhu C (2006) Electron microbeam investigation of uranium-contaminated soils from oak ridge, TN, USA. Environ Sci Technol 40:2108–2113
28. Liu M, Dong F, Wei Z, Nie X, Sun S, Wei H, Lang L, Sha X, Zhang G (2016) Programmed gradient descent biosorption of strontium ions by *Saccaromyces cerevisiae* and ashing analysis: a decrement solution for nuclide and heavy metal disposal. J Hazard Mater 314:295–303
29. Stearn AE, Stearn EW (1928) Studies in the physico-chemical behavior of bacteria. A Quarterly of Research, University of Missouri Studies
30. Bampaiti A, Yusan S, Aytas S, Pavlidou E, Noli F (2016) Investigation of uranium biosorption from aqueous solutions by *Dictyopteris polypodioides* brown algae. J Radioanal Nucl Chem 307:1335–1343
31. Kulkarni S, Misra CS, Gupta A, Ballal A, Apte SK (2016) Interaction of uranium with bacterial cell surfaces: inferences from phosphatase-mediated uranium precipitation. Appl Environ Microbiol 82:4965–4974
32. Panak P, Raff J, Selenska-Pobell S, Geipel G, Bernhard G, Nitsche H (2000) Complex formation of U(VI) with *Bacillus*-isolates from a uranium mining waste pile. Radiochim Acta 88:71–76

33. Haas JH, Dichristina TJ, Wade R (2001) Thermodynamics of U(VI) sorption onto *Shewanella putrifaciens*. Chem Geol 180:33–54
34. Gorman-Lewis D, Elias PE, Fein JB (2005) Adsorption of aqueous uranyl complexes onto *Bacillus subtilis* cells. Environ Sci Technol 39:4906–4912
35. Osmond F (1887) Dosage colorimétrique du phosphore. Bull Soc chim (Paris) 47:745–748
36. Nie X, Dong F, Liu N, Liu M, Zhang D, Kang W, Sun S, Zhang W, Yang J (2015) Subcellular distribution of uranium in the roots of *Spirodela punctata* and surface interactions. Appl Surf Sci 347:122–130
37. Krawczyk-Bärsch E, Lütke L, Moll H, Bok F, Steudtner R, Rossberg A (2015) A spectroscopic study on U(VI) biomineralization in cultivated *Pseudomonas fluorescens* biofilms isolated from granitic aquifers. Environ Sci Pollut R 22:4555–4565
38. Beazley MJ, Martinez RJ, Sobecky PA, Webb SM, Taillefert M (2007) Uranium biomineralization as a result of bacterial phosphatase activity: insights from bacterial isolates from a contaminated subsurface. Environ Sci Technol 41:5701–5707
39. Macaskie LE, Bonthrone KM, Yong P, Goddard DT (2000) Enzymically mediated bioprecipitation of uranium by a *Citrobacter* sp.: a concerted role for exocellular lipopolysaccharide and associated phosphatase in biomineral formation. Microbiology 146:1855–1867
40. Beazley MJ, Martinez RJ, Sobecky PA, Webb SM, Taillefert M (2009) Nonreductive biomineralization of uranium(VI) phosphate via microbial phosphatase activity in anaerobic conditions. Geomicrobiol J 26:431–441
41. Sousa T, Chung AP, Pereira A, Piedade AP, Morais PV (2013) Aerobic uranium immobilization by Rhodanobacter A2-61 through formation of intracellular uranium-phosphate complexes. Metallomics 5:390–397
42. Martinez RJ, Beazley MJ, Taillefert M, Arakaki AK, Skolnick J, Sobecky PA (2007) Aerobic uranium(VI) bioprecipitation by metal-resistant bacteria isolated from radionuclide- and metal-contaminated subsurface soils. Environ Microbiol 9:3122–3133
43. Suzuki Y, Banfield JF (2004) Resistance to, and accumulation of uranium by bacteria from a uranium-contaminated site. Geomicrobiology 21:113–121
44. Riba O, Scott TB, Vala Ragnarsdottir K (2008) Reaction mechanism of uranyl in the presence of zero-valent iron nanoparticles[J]. Geochim Cosmochim Acta 72(16):4047–4057
45. Acharya C, Joseph D, Apte SK (2009) Uranium sequestration by a marine cyanobacterium, *Synechococcus elongatus* strain BDU/75042. Bioresour Technol 100:2176–2181
46. Soylak M, Khan M, Alosmanov R, Shah J, Jan MR (2016) Solid phase extraction of uranium(VI) on phosphorus-containing polymer grafted 4-aminoantipyrine. J Radioanal Nucl Chem 308:955–963
47. Alessi DS, Lezama-Pacheco JS, Stubbs JE, Janousch M, Bargar JR, Persson P, Bernier-Latmani R (2014) The product of microbial uranium reduction includes multiple species with U(IV)–phosphate coordination. Geochim Cosmochim Acta 131:115–127
48. Müller K, Brendler V, Foerstendorf H (2008) Aqueous uranium(VI) hydrolysis species characterized by attenuated total reflection fourier-transform infrared spectroscopy. Inorg Chem 47:10127–10134
49. Duff MC, Coughlin JU, Hunter DB (2002) Uranium co-precipitation with iron oxide minerals. Geochim Cosmochim Acta 66:3533–3547
50. Wazne M, Korfiatis GP, Meng X (2003) Carbonate effects on hexavalent uranium adsorption by iron oxyhydroxide. Environ Sci Technol 37:3619–3624
51. Müller K, Foerstendorf H, Meusel T, Brendler V, Lefèvre G, Comarmond MJ, Payne TE (2012) Sorption of U(VI) at the TiO_2–water interface: an in situ vibrational spectroscopic study. Geochim Cosmochim Acta 76:191–205
52. Yu D, Bo B, Yunhua H (2013) Fabrication of TiO2@Yeast-carbon hybrid composites with the raspberry-like structure and their synergistic adsorption-photocatalysis performance. J Nanomater 2013:4053–4062
53. Paterson-Beedle M, Readman JE, Hriljac JA, Macaskie LE (2010) Biorecovery of uranium from aqueous solutions at the expense of phytic acid. Hydrometallurgy 104:524–528
54. Pan X, Chen Z, Chen F, Cheng Y, Lin Z, Guan X (2015) The mechanism of uranium transformation from U(VI) into nano-uramphite by two indigenous *Bacillus thuringiensis* strains. J Hazard Mater 297:313–319